Supplemental material

Barro-Soria, https://doi.org/10.1085/jgp.201812221

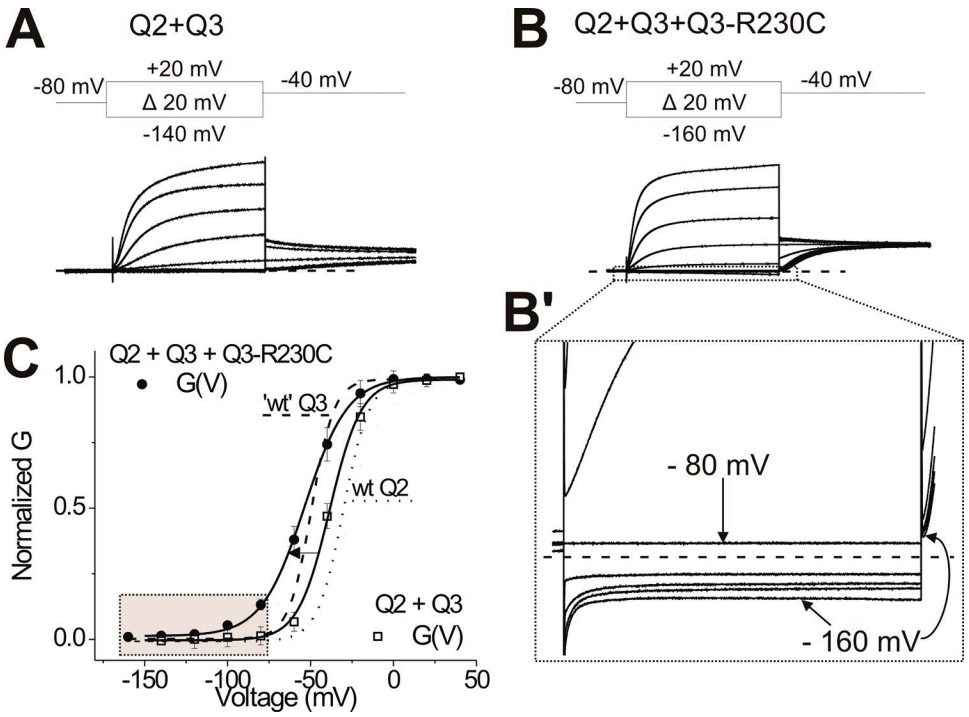

Figure S1. **Heteromeric channels incorporating the epilepsy-causing mutation R230C shift the voltage dependence of channel gating to more negative voltages compared with WT KCNQ2/KCNQ3. (A and B)** Representative current from heteromeric KCNQ2/KCNQ3 (A) and KCNQ2/KCNQ3/KCNQ3-R230C (B) channels (coexpressed at a ratio of 2:1:1) for the indicated voltage protocol. **(B′)** The enlarged current trace from B shows a fraction of constitutive current at strong hyperpolarized voltages. Dashed lines in A, B, and B′ represent zero current. **(C)** Normalized $G(V)$ curves of recordings from KCNQ2/KCNQ3 (square) and KCNQ2/KCNQ3/KCNQ3-R230C (circles) channels (means ± SEM; n = 7–11). Lines represent the fitted theoretical voltage dependencies (see Materials and methods, Eqs. 1 and 2). The $G(V)$ curves (from Boltzmann fit) from KCNQ3-A315T (dashed line) and KCNQ2 (dotted line) channels are shown for comparison. Dashed gray rectangle is shown to highlight differences in steady-state conductance between KCNQ2/KCNQ3 and KCNQ2/KCNQ3/KCNQ3-R230C from −160 mV to −80 mV.

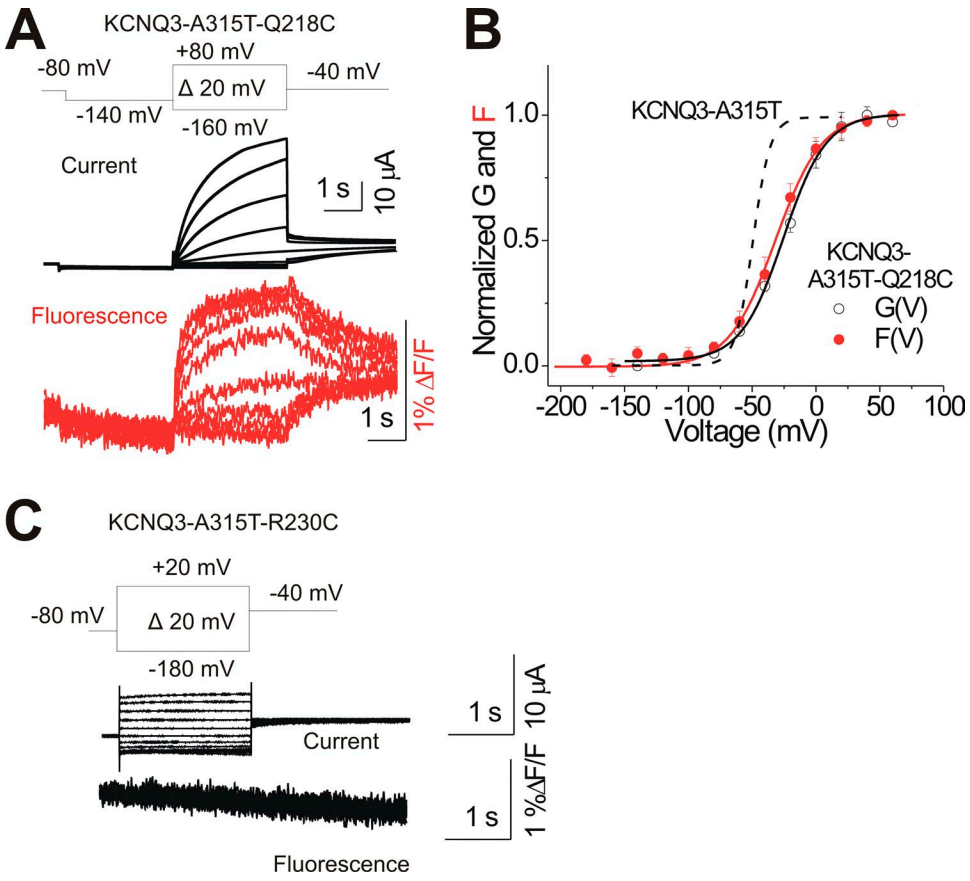

Figure S2. **Voltage-dependent fluorescence signals from KCNQ3-A315T-Q218C channels. (A)** Representative current (black) and fluorescence (red) from Alexa Fluor 488–labeled KCNQ3-A315T-Q218C channels for the indicated voltage protocol. **(B)** Normalized *G*(*V*) (black) and *F*(*V*) (red) curves of recordings from KCNQ3-A315T-Q218C channels (means ± SEM; *n* = 10). Lines represent the fitted theoretical voltage dependencies (see Materials and methods, Eqs. 1 and 2). The *G*(*V*) (dashed line) curve (from Boltzmann fit) of KCNQ3-A315T channels is shown for comparison. **(C)** Representative current (top panel) and fluorescence (bottom panel) from KCNQ3-A315T-R230C channels incubated with Alexa Fluor 488 5-maleimide for the indicated voltage protocol and under the same experimental condition as in A (see Materials and methods).

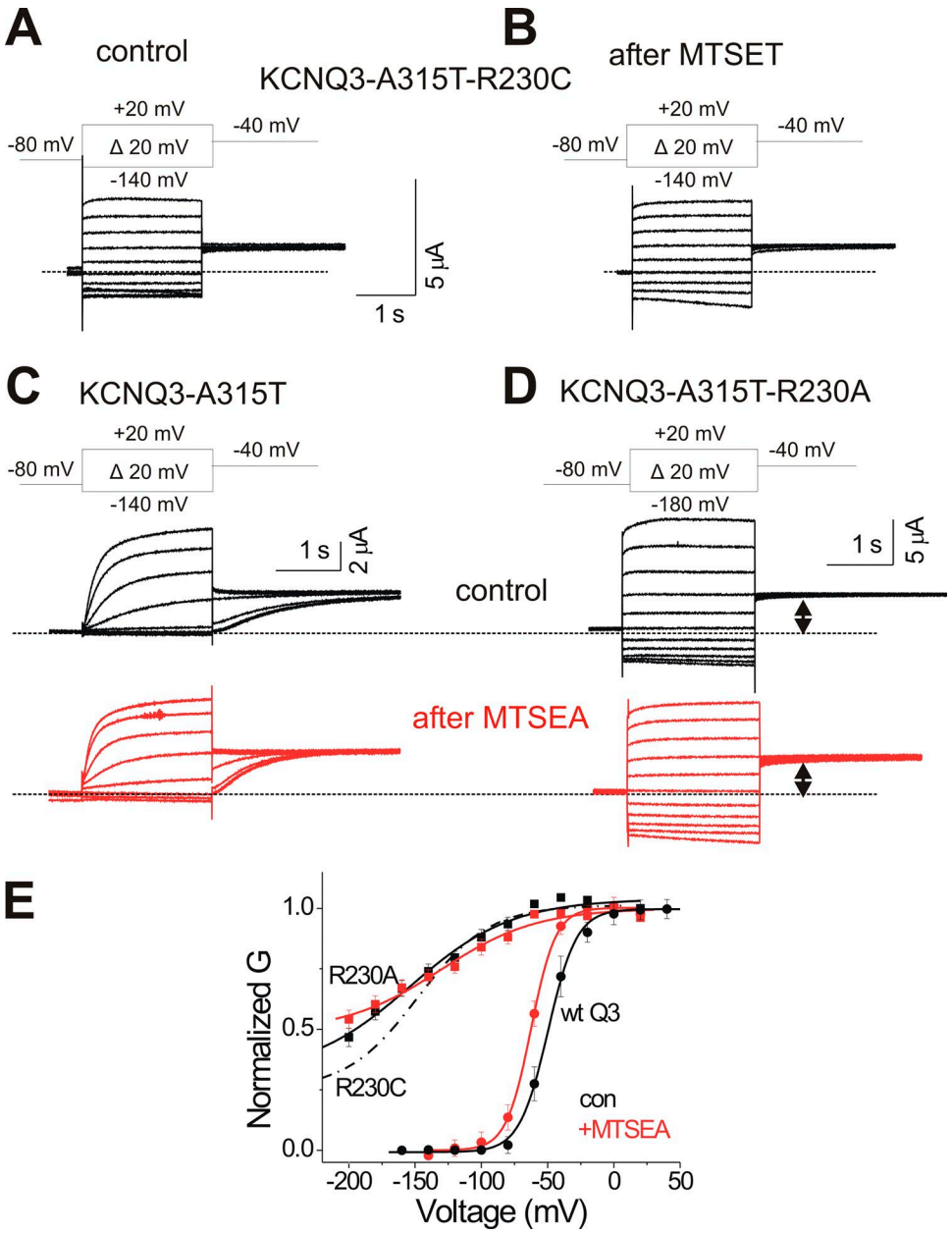

Figure S3. **Membrane-permeable thiol MTS reagents do not modify either WT KCNQ3 or KCNQ3 bearing R230A mutant. (A and B)** Representative current traces from KCNQ3-A315T-R230C channels before (A) and after (B) application of 10 µM MTSET for the indicated voltage protocols. **(C and D)** Representative current traces from KCNQ3-A315T (C) and KCNQ3-A315T-R230A (D) channels before (black) and after (red) application of 1 mM MTSEA for the indicated voltage protocols. MTSET and MTSEA were applied by stepping 15 times to +20 mV for 5 s, from a holding voltage of −80 mV, and then washed away for 15 s, before the indicated voltage protocol was applied. Dashed lines represent zero current. **(E)** Normalized *G*(*V*) curves of recordings from KCNQ3-A315T (WT Q3) and KCNQ3-A315T-R230A channels before (black lines) and after (red lines) application of MTSEA (means ± SEM; $n = 8$). For comparison, the *G*(*V*) curve (dashed line) of KCNQ3-A315T-R230C channel is shown.

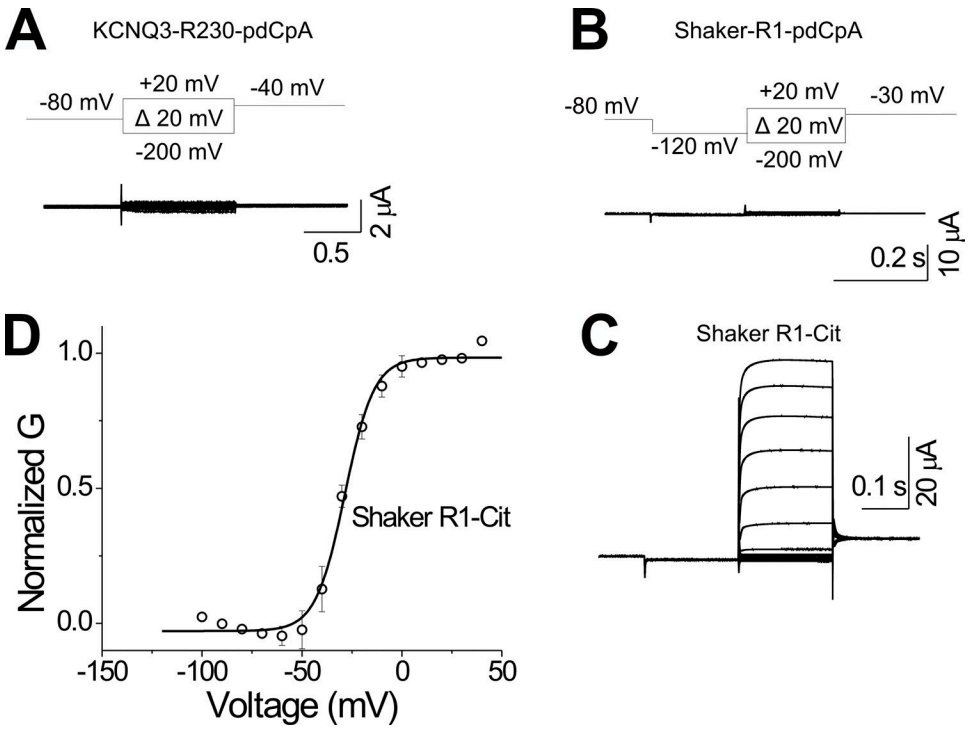

Figure S4. **Encoding of the noncanonical amino acid citrulline in Shaker R362UAG channel. (A–C)** Representative current traces from KCNQ3-R230UAG + Pyl-pdCpA (A), Shaker-R362UAG + Pyl-pdCpA (B), and Shaker-362Citrulline (R1Cit; C) channels for the indicated voltage protocols. **(D)** Normalized *G*(*V*) curve from Shaker-R1Cit channels. Each control experiment was repeated at least 10 times (means ± SEM) in the same batch of *Xenopus* oocytes.